ASM | Journal of Bacteriology

Check for updates

| Editor's Pick | Bacteriology | Full-Length Text

High levels of antisense transcription from numerous genes in the obligate intracellular bacterium *Orientia tsutsugamushi*

Chitrasak Kullapanich,[1] Regan Hayward,[2] Lars Barquist,[2,3,4] Jeanne Salje[1,5,6,7]

AUTHOR AFFILIATIONS See affiliation list on p. 14.

ABSTRACT *Orientia tsutsugamushi* (Ot) is a cytoplasmic, gram-negative, obligate intracellular bacterium that causes the human disease scrub typhus. It has a highly repetitive genome, whereby approximately 50% is composed of multiple copies of a proliferated integrative and conjugative element, the Rickettsial amplified Genetic Element (RAGE). Previous RNA sequencing analysis revealed a high level of antisense transcription in Ot, particularly from RAGE-encoded genes, with 18% of all genes having a sense:antisense ratio <1 and 5% with a ratio <0.1. In our current study, we have confirmed the earlier RNA sequencing findings via polymerase chain reaction (PCR)-based methods and established that this antisense transcription is a consistent feature across eight distinct Ot strains. Furthermore, we have utilized PCR to monitor differences in sense and antisense expression between intracellular and extracellular bacteria. Our findings lend weight to the hypothesis that antisense transcription in Ot is a regulated mechanism, possibly playing a crucial role in the pathogen's lifecycle during infection.

IMPORTANCE *Orientia tsutsugamushi* (Ot) is an obligate intracellular bacterium with a highly repetitive genome and an unusual abundance of antisense RNA transcripts. Antisense transcription has been proposed to regulate gene expression, yet its biological significance in intracellular bacteria remains unclear. By confirming high and conserved levels of antisense transcription in specific genes across multiple *O. tsutsugamushi* strains and showing that antisense expression decreases in extracellular forms, this study provides new evidence that antisense transcription is a regulated process rather than transcriptional noise. These findings suggest that antisense RNAs may play a role in controlling gene activity during the bacterial life cycle, offering insights into gene regulation in organisms with reduced and repetitive genomes.

KEYWORDS *Orientia tsutsugamushi*, antisense transcription, RNA sequencing, obligate intracellular bacteria, Rickettsiales

Orientia tsutsugamushi (Order Rickettsiales, Family Rickettsiaceae) (Ot) is an obligate intracellular gram-negative alphaproteobacterium that causes the mite-borne human disease scrub typhus (1, 2). This is endemic in many parts of rural Asia, with related species causing scrub typhus-like illness recently reported from Latin America (3, 4) and the Middle East (5). Symptoms begin 7–10 days after being bitten by an infected mite and include headache, fever, rash, and a distinctive lesion called an eschar at the site of inoculation. If not treated with timely administration of effective antibiotics, the infection can escalate to cause multiple organ failure and death, with a median mortality of 6% in untreated cases (6).

Ot is an obligate intracellular bacterium that escapes from the endolysosomal pathway shortly after cellular internalization and carries out its growth and replication directly in the eukaryotic cytoplasm (7, 8). It traffics to the perinuclear region using dynein-dependent motility (9) mediated by the bacterial surface autotransporter protein

Editor Michael Y. Galperin, National Institutes of Health, Bethesda, Maryland, USA

Address correspondence to Jeanne Salje, jss53@cam.ac.uk.

The authors declare no conflict of interest.

See the funding table on p. 14.

Received 2 December 2025
Accepted 16 July 2026
Published 12 August 2026

Copyright © 2026 Kullapanich et al. This is an open-access article distributed under the terms of the Creative Commons Attribution 4.0 International license.

Downloaded from https://journals.asm.org/journal/jb on 21 August 2026 by 131.111.184.205.

Downloaded from https://journals.asm.org/journal/jb on 21 August 2026 by 131.111.184.205.

ScaC (10), where it undergoes replication within a tightly packed bacterial microcolony. Following replication, Ot exits infected cells using a budding mechanism, in which it buds off the surface encased in the host plasma membrane (11–13). The stability of the plasma membrane around extracellular bacteria and its role in immune evasion and subsequent cell infection are unknown. Ot differentiates into a distinct form prior to bacterial exit, and the intracellular (IB) and extracellular (EB) forms of Ot exhibit different protein profiles, morphology, and peptidoglycan abundance (14). The mechanisms by which gene expression is regulated across the different stages of the infection cycle are unknown, although global transcript levels are low in the extracellular state, likely reflecting its metabolically inactive state resulting from a lack of access to nutrients in the host cell cytoplasm (14). However, the relative sense transcript levels in IB and EB forms of Ot are different across different genes, reflecting differentially regulated transcription between these states (14). Relative levels of antisense transcripts across different stages of the Ot infection cycle have not been reported to date.

Ot has an unusual genome that is characterized by rampant proliferation of mobile genetic elements (15–17). Dominant among these is the Rickettsial Amplified Genetic Element (RAGE), which is present in 70–90, mostly degraded, copies across the bacterial genome (18). While this RAGE is present in some species of the sister genus *Rickettsia* (19–24), the scale of amplification is unmatched in other described organisms. It is now known that at least some Ot strains encode intact, full-length RAGEs (18), suggesting that active movement of this element may still be ongoing at the population level, but the dynamics of the Ot genome remains to be determined.

Antisense transcription can regulate genes through *cis* or *trans* activity, in which it binds to the opposite-strand mRNA transcribed from the same gene or a gene located elsewhere on the genome, respectively. The *trans*-active antisense small RNAs tend to interact with multiple targets, with a lower degree of sequence specificity, while *cis*-acting antisense transcripts have perfect sequence complementarity to the opposite-strand mRNA. Antisense transcripts can regulate gene expression by blocking translation or causing RNAse III-dependent degradation of double-stranded RNA. Functional antisense transcription in prokaryotes was originally described in bacteriophages and transposases, where they were shown to control the expression levels of these potentially damaging elements (25, 26). For example, *cis*-binding antisense RNA leads to degradation of the mRNA encoding a transposase gene, thus controlling transposon movement in the *S. flexneri* R100 plasmid (27, 28), while binding of an antisense RNA at the ribosomal binding site of the anti-repressor protein Ant blocks the switch to lytic growth of *Salmonella* P22 phage (29). More recently, pervasive antisense transcription has been described in numerous bacterial species including *E. coli, Helicobacter pylori, Bacillus subtilis, Vibrio cholerae, Chlmaydia trachomatis, Pseudomonas syringae,* and *Mycobacterium tuberculosis* (26, 30). RNA sequencing has revealed that many bacterial genomes express antisense transcription, but it can be difficult to determine whether these result from spurious, nonspecific antisense transcription initiation or the activity of specific, cryptic antisense promoters. It has been shown that the level of genome-wide antisense transcription correlates positively with the genomic AT content (31), which can be explained by the fact that the Pribnow motif in bacterial promoters has the consensus sequence "5′-TANAAT-3′," so spurious promoters are much more likely in AT-rich genomes. Ultimately, the biological activity of an antisense transcript can be determined experimentally through gene modification, but this is more difficult to achieve in the case of *cis*-acting transcripts where the antisense transcript cannot easily be destroyed without affecting the coupled sense transcript.

We previously carried out a dual RNA sequencing analysis of Ot strains Karp and UT176 grown in cultured human umbilical endothelial cells (HUVECs) in which both bacterial and host transcript abundances were determined (32). High levels of bacterial antisense transcription were observed, with up to 1,000-fold enrichment of *cis* antisense transcripts compared to protein-coding, sense transcripts for some genes. Genes with low sense:antisense ratios were enriched in the RAGE mobile genetic element

regions, and these genes were also associated with a lack of detectable peptides in a shotgun proteomics analysis carried out in parallel. That finding suggested that antisense transcription may be associated with decreased translation either through degradation of the associated mRNA or through decreased ribosome accessibility, leading to decreased protein synthesis. One limitation of that study was that we did not independently measure antisense transcripts using alternative techniques and could not completely rule out the high levels of transcription being due to an artifact of the RNA sequencing approach used. A second limitation was that at that time, the RAGE genes were not well annotated, and we, therefore, did not carry out a detailed analysis of the identity of RAGE genes with high antisense transcription. A new study reporting reannotation of eight Ot genomes (18) has enabled us to perform such analysis in the current work.

Here, we sought to explore the biological significance of previously described antisense *cis* RNA transcription in Ot. We reasoned that a conserved pattern of antisense expression across different Ot strains would indicate the presence of a specific antisense promoter and its potential role in bacterial growth and pathogenicity. We analyzed genome-wide antisense transcription across eight related strains of Ot and found that antisense transcription is highly regulated between strains, with some genes exhibiting conserved patterns of antisense transcription along the length of the gene, indicative of a specific transcription start site. We carried out PCR analysis of both sense and antisense transcription of six genes in one Ot strain, the clinical isolate Karp, and found that the trends in sense:antisense ratios broadly replicated that measured by RNA sequencing. We then compared the sense:antisense ratio at different stages of the infection cycle and observed a reduction in antisense transcripts in extracellular Ot.

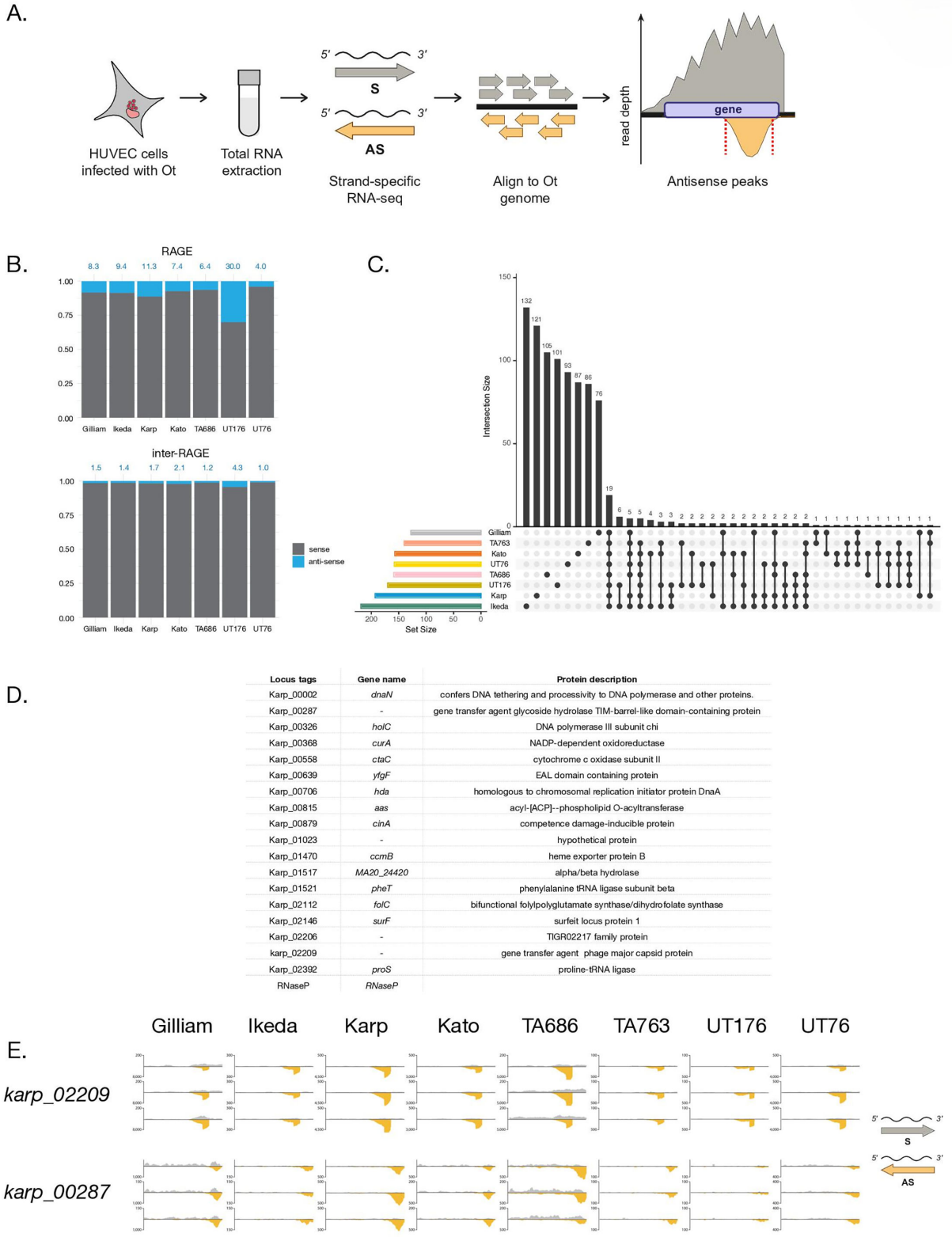
RESULTS

High antisense transcription is conserved across diverse Ot strains

Antisense transcription has previously only been described in two Ot strains: Karp and UT176. We asked whether the presence of genes with high antisense transcription was universal across diverse Ot strains and whether a comparative analysis could identify individual genes with consistently high antisense transcription. We carried out a dual RNA sequencing experiment in which seven Ot strains, Gilliam, Ikeda, Karp, Kato, TA686, and UT76, were grown for 5 days in human umbilical vein endothelial cells (HUVECs). The results of that analysis have been reported elsewhere (33). In the current study, we reanalyzed this data set, together with a previous analysis of Karp and UT176 (32), to give a total of eight different strains, with a particular focus on the distribution of genes with high levels of antisense transcription. First, we compared the levels of antisense transcription in both coding and, where annotated, noncoding regions in the multi-copy RAGE integrative and conjugative element with those in the inter-RAGE (IR) regions (Fig. 1B). We found that all strains exhibited higher levels of antisense transcription in RAGE genes compared with IR genes, consistent with previous reports (32). Between 1% and 4.3% of all inter-RAGE reads and 4% and 30% of all RAGE reads mapped to genes in the antisense orientation. While this was a significant level of antisense transcription, it was lower than the levels reported by us previously (32). This is likely to reflect differences in library preparation protocols, with the previous methodology specifically optimized for capturing both shorter transcripts and long (mRNA) transcripts. The relative abundance of antisense transcripts in different strains did not correlate with phylogeny (18) or relative virulence (10). We performed peak calling on antisense reads (see *Methods*) to identify discrete antisense transcripts overlapping coding and noncoding genes and determined a cut-off of 200 reads to classify genes as expressing high levels of antisense transcription and quantified the high antisense genes present in single strains or groups of strains across all conserved genes (Fig. 1C). The mean width of antisense peaks was 435 nucleotides in Karp as a representative example, with the shortest antisense to a coding sequence being 93 bases and the longest 1,599 bases. Nineteen genes were identified as having high antisense transcript levels in all eight

Downloaded from https://journals.asm.org/journal/jb on 21 August 2026 by 131.111.184.205.

Downloaded from https://journals.asm.org/journal/jb on 21 August 2026 by 131.111.184.205.



Locus tags	Gene name	Protein description
Karp_00002	*dnaN*	confers DNA tethering and processivity to DNA polymerase and other proteins.
Karp_00287	-	gene transfer agent glycoside hydrolase TIM-barrel-like domain-containing protein
Karp_00326	*holC*	DNA polymerase III subunit chi
Karp_00368	*curA*	NADP-dependent oxidoreductase
Karp_00558	*ctaC*	cytochrome c oxidase subunit II
Karp_00639	*yfgF*	EAL domain containing protein
Karp_00706	*hda*	homologous to chromosomal replication initiator protein DnaA
Karp_00815	*aas*	acyl-[ACP]--phospholipid O-acyltransferase
Karp_00879	*cinA*	competence damage-inducible protein
Karp_01023	-	hypothetical protein
Karp_01470	*ccmB*	heme exporter protein B
Karp_01517	*MA20_24420*	alpha/beta hydrolase
Karp_01521	*pheT*	phenylalanine tRNA ligase subunit beta
Karp_02112	*folC*	bifunctional folylpolyglutamate synthase/dihydrofolate synthase
Karp_02146	*surF*	surfeit locus protein 1
Karp_02206	-	TIGR02217 family protein
karp_02209	-	gene transfer agent phage major capsid protein
Karp_02392	*proS*	proline-tRNA ligase
RNaseP	*RNaseP*	

FIG 1 A comparison of antisense transcription across eight diverse Ot strains. An RNA sequencing analysis was carried out on eight diverse Ot strains grown in cultured human umbilical vein endothelial cells (HUVECs). (A) Schematic overview of the workflow. (B) Quantification of the percentage of sense and antisense transcripts from the total number of reads in each strain, separated by genes encoded in RAGE and IR regions of the bacterial genome. All strains exhibit

(Continued on next page)

Fig 1 (Continued)

higher antisense transcription from RAGE genes. (C) A comparison of the number of high-antisense genes across genomes. Bars demonstrate the number of high-antisense genes present in individual strains and combinations of strains, as indicated by the black dots below each column. Nineteen genes have high antisense transcription in all eight strains. (D) Description of the 19 genes with high levels of antisense transcription in all Ot strains. (E) Transcript maps showing the distribution of sense and antisense reads in the raw RNA sequencing data across three biological replicates for two gene transfer agent genes with high antisense transcripts, Karp_02209 and Karp_00287. Sense transcripts are shown in gray, and antisense transcripts are shown in yellow. The exact positions of transcripts are given in Tables S4 to S11.

strains, and these are listed in Fig. 1D. The conservation of antisense transcription across strains suggests that the antisense RNAs associated with these 19 genes are regulated and potentially functional, whereas much of the remaining antisense transcription across the Ot genome may arise from pervasive, nonspecific transcription. Of the 19 genes with conserved antisense transcripts, two encoded genes in the phage-like gene transfer agent recently identified in Ot: Karp_02209 encoding the major capsid protein and Karp_00287 encoding the tail protein. This is consistent with the described regulation of phage DNA by antisense transcription (27–29). A comparison of the sequencing reads of these two genes across three biological replicates and eight Ot strains reveals that both genes encode a single, conserved region of high antisense transcription at the 3′ end of the gene (Fig. 1E). This high conservation suggests the potential presence of a specific antisense promoter in this region, as described for other well-defined bacterial antisense transcripts (34, 35).

Design of a PCR assay to measure antisense transcription in Ot

We sought to validate the RNA sequencing data using an independent PCR-based experimental approach. First, we used the RNA sequencing data to select six genes with high (*ftsZ, ctrA,* and *spoT*) and low (*ank12_01, folC,* and *scaD*) sense:antisense transcript ratios (Fig. 2A). *folC* exhibits a single antisense peak at the 3′ end of the sense transcript that is conserved across all strains and biological replicates. By contrast, *ank12_01* exhibits a peak toward the middle of the gene that is not present in all strains, as well as other antisense peaks present in only some strains and replicates. *scaD* exhibits two peaks, one in the middle of the gene and one at the 3′ end of the sense strand, but these are not both universally present in all strains. Based on the RNA sequencing data, we expect *folC* to exhibit the highest and most robust antisense:sense ratio.

We sought to confirm the presence of antisense RNA transcripts observed in the RNA-seq data using Northern blot analysis. We designed probes corresponding to predicted antisense peaks in the gene transfer agent genes *karp_00287* and *karp_02209,* as well as genes *ank12_01, folC,* and *scaD* (Fig. S1; Table S3). We observed strong bands corresponding to antisense transcripts in genes *karp_00287, karp_02209, ank12_01,* and *scaD,* although in all genes other than *karp_00287,* the band was of a larger size than expected (Fig. 2B). No band could be detected for the gene *folC*.

We designed a PCR-based assay to selectively amplify sense or antisense transcripts (Fig. 3A). We used individual primers that would only amplify sense or antisense transcripts during the reverse transcription step, followed by nested PCR amplification of cDNA. A single sense primer was designed with a binding region at the 3′ end of the gene. Since antisense transcripts do not necessarily cover the full length of the gene, we designed multiple antisense primers that would reverse-transcribe RNA from different regions of the gene. The primers used for each gene are shown in Fig. 3B. In the case of genes with substantial antisense transcription predicted (Fig. 2), we designed primers covering both the specific regions with local antisense peaks and other regions across the gene.

Downloaded from https://journals.asm.org/journal/jb on 21 August 2026 by 131.111.184.205.

Downloaded from https://journals.asm.org/journal/jb on 21 August 2026 by 131.111.184.205.

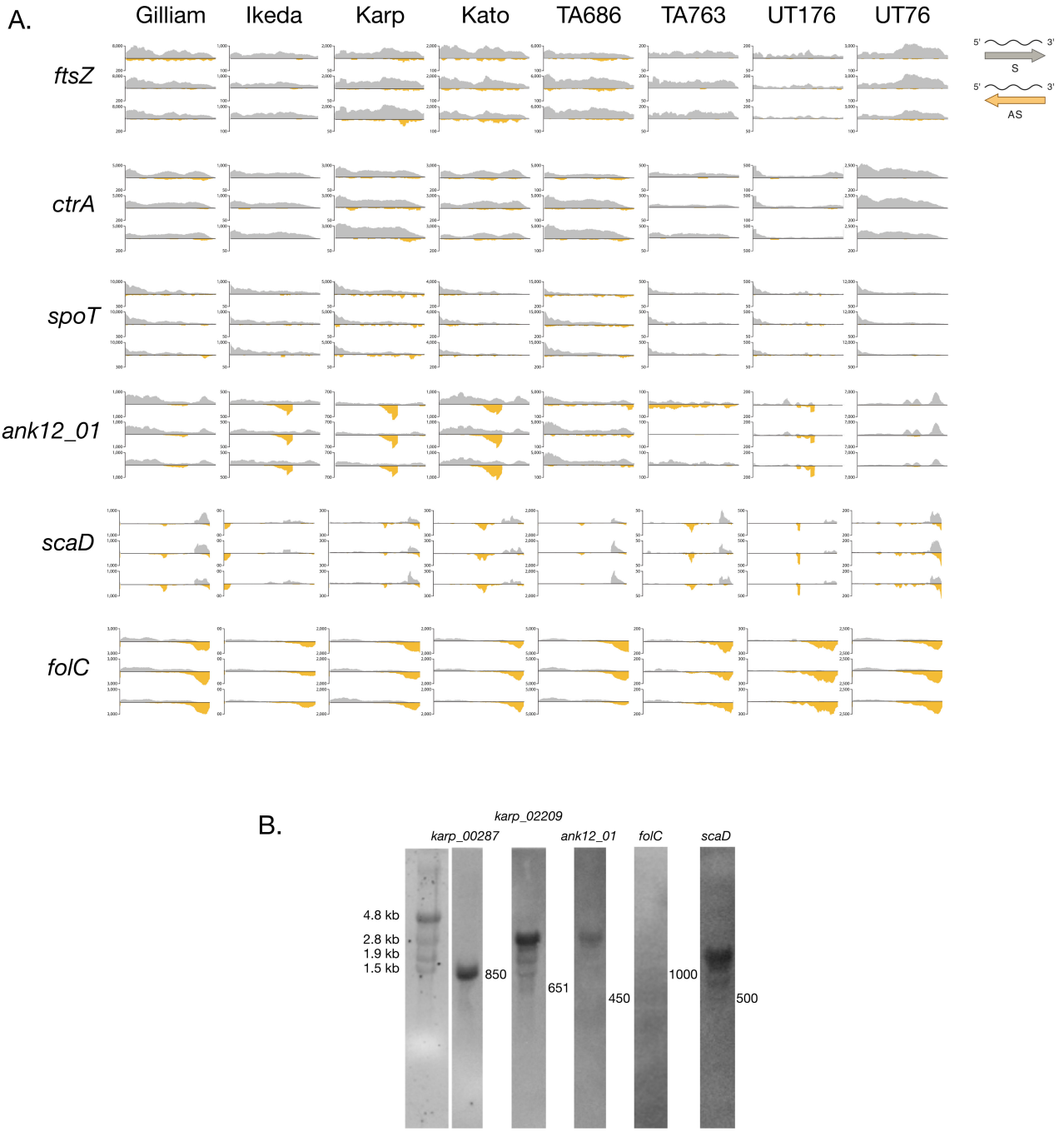


FIG 2 Antisense transcription across six Ot genes. (A) Transcript maps showing the distribution of sense and antisense reads in the raw RNA sequencing data across three biological replicates for six selected Ot genes. Sense transcripts are shown in gray, and antisense transcripts are shown in yellow, and all genes are oriented in the sense direction irrespective of their orientation in the genome. *ftsZ, ctrA,* and *spoT* exhibit low antisense transcription, while *ank12_01, folC,* and *scaD* exhibit high antisense transcription. The exact positions of transcripts are given in Tables S4 to S11. (B) Northern blot data demonstrating the presence of antisense transcripts in *karp_00287, karp_02209, ank12_01,* and *scaD*. These analyses were carried out on RNA isolated from L929 at 5 days post-infection. Additional data demonstrating sample and probe preparation are given in Fig. S1.

Downloaded from https://journals.asm.org/journal/jb on 21 August 2026 by 131.111.184.205.

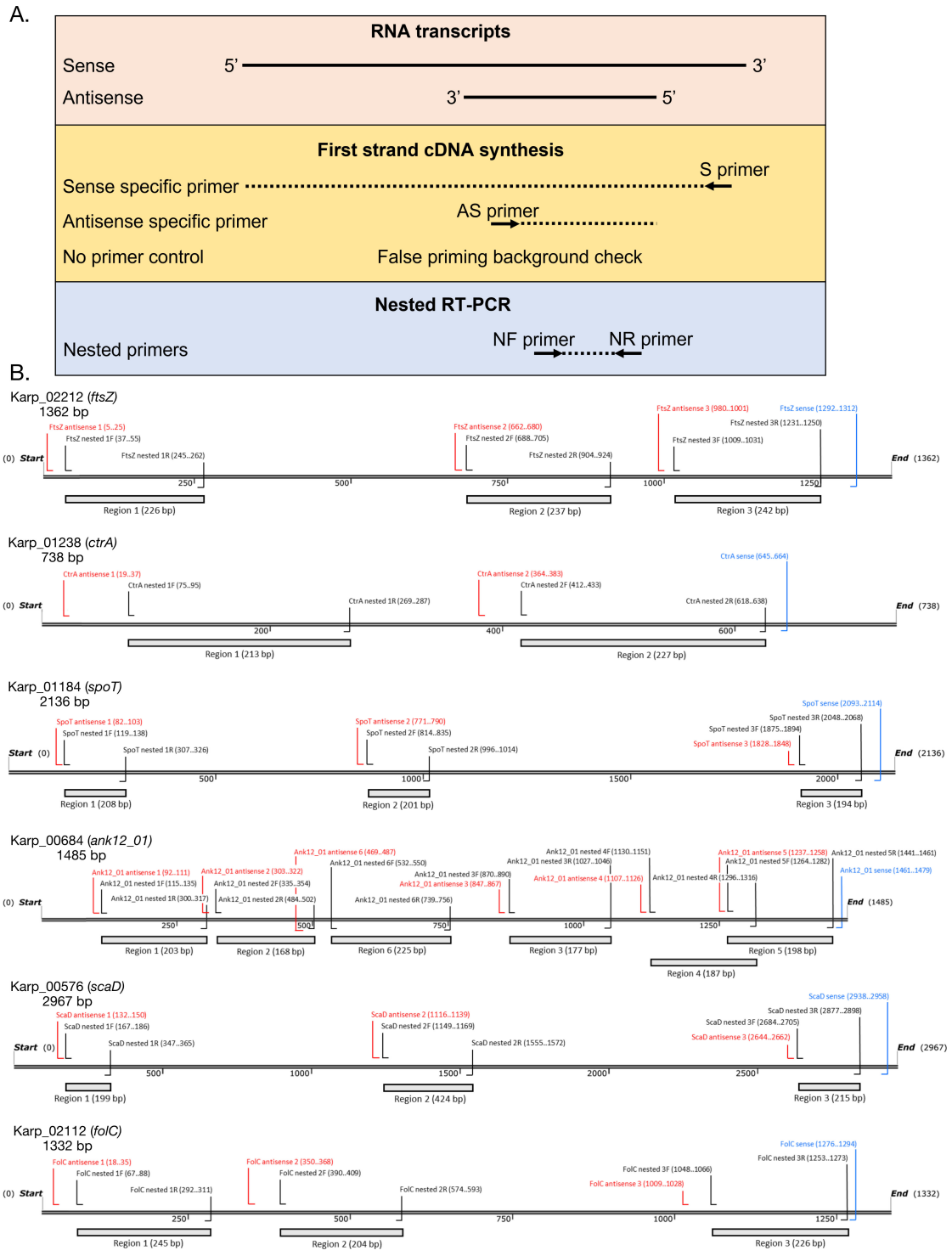


FIG 3 PCR assay to measure antisense transcription. (A) Design of PCR assay to quantify relative levels of sense and antisense transcription. (B) Gene maps showing the primers used to measure sense and antisense transcripts at multiple positions across six Ot genes.

PCR-based quantification of sense and antisense transcripts confirms different antisense:sense ratios between six Ot genes

We used the sense:antisense PCR assay to quantify transcript levels of Ot grown in mouse fibroblast L929 cells. We used a different cell line from the human umbilical vein endothelial (HUVEC) cells used in the RNA sequencing data so that we could explore

Downloaded from https://journals.asm.org/journal/jb on 21 August 2026 by 131.111.184.205.

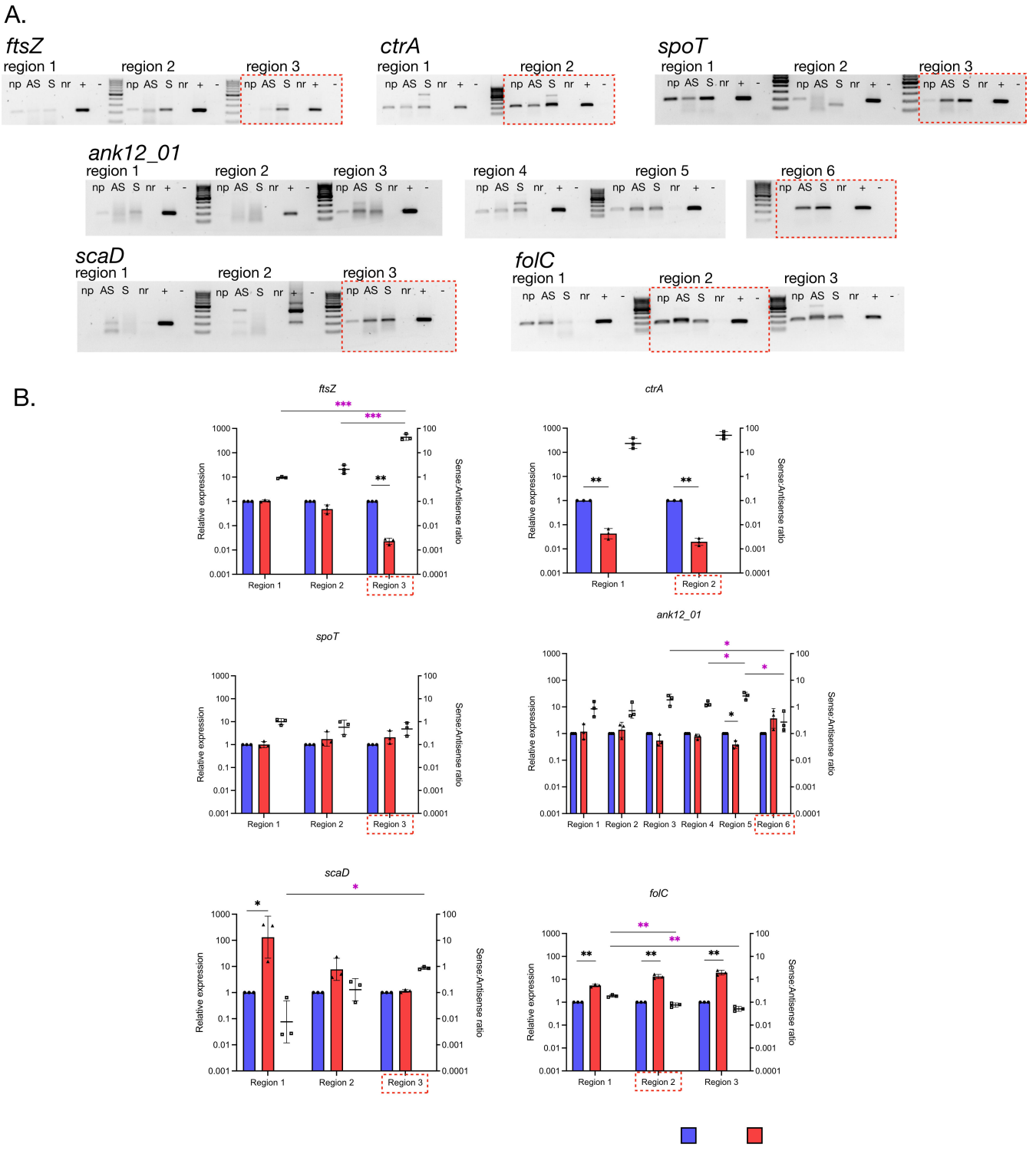


FIG 4 Quantification of the sense/antisense ratio at different regions within each gene. (A) DNA gels showing results of PCRs carried out using primers shown in Fig. 3B. np = no primer used during cDNA synthesis, AS = results using antisense primer, S = results using sense primer, nr = no reverse transcriptase, + = positive control using Ot genomic DNA, − = negative control using nuclease-free water in place of DNA. A 100-bp molecular weight marker was used. The region used in subsequent experiments presented in Fig. 5 are indicated with a red dotted line. (B) Graphs showing quantification of the relative expression of sense and antisense transcripts using the same primers as in Fig. 3B. Expression was measured using RT-qPCR, and transcript levels were normalized to the Ot DNA copy number. Graph shows the relative expression on the left y-axis, and the sense:antisense ratio for each region is shown on the right y-axis. The results of three independent replicates are shown. Graph shows mean and standard deviation. Statistical significance was determined using a standard *t* test with Welch

(Continued on next page)

Fig 4 (Continued)

correction, where ns indicates no significant difference, * indicates *P*-value ≤ 0.05, ** *P*-value ≤ 0.01, and *** *P*-value ≤ 0.01. The black asterix compares relative expression, while the magenta asterix compares the sense:antisense ratio. The regions used in subsequent experiments presented in Fig. 5 are indicated with a red dotted line.

the universality of our findings. RNA was isolated from intracellular bacteria grown for 4 days post-infection, and the relative levels of sense and antisense transcripts were measured by PCR and RT-qPCR, respectively (Fig. 4A and B). We observed substantial differences between the primers designed to amplify different regions of the gene, in terms of their amplification of nonspecific RNA in the no priming control as well as the relative levels of sense and antisense transcription. Broadly, our results supported the predictions based on RNA sequencing data. All primer pairs against *ftsZ* and *ctrA* exhibited a sense:antisense ratio >1, while for *spoT, ank12_01,* and *scaD,* the genes were shown to have weak and/or variable antisense peaks and the sense:antisense ratio was close to 1. Finally, for the gene *folC* that was shown to have a strong and conserved antisense peak, the level of antisense was higher than that of the sense in all three regions tested, with a ratio of up to 0.1. Region 3 corresponds to the region covering the antisense peak observed in the RNA sequencing data. While this region exhibited a lower sense:antisense ratio than the other two, all three regions exhibit substantial antisense transcription.

We selected one region for each gene, highlighted by a red dotted line in Fig. 4A, for subsequent analysis. These regions were selected based on the presence of antisense transcripts (where present) in RNA sequencing data and RT-qPCR analysis as well as clear amplification of a single PCR product.

Antisense transcription is reduced in extracellular bacteria

Ot exhibits a developmental cycle in which IB form Ot is replicative and translationally active, while EB Ot does not replicate and is translationally inactive. Both forms are infectious. We asked whether the sense:antisense ratio would vary between these two bacterial forms. RNA was isolated from both IB and EB Ot grown in L929 cells for 5 and 7 days, and the relative levels of sense and antisense transcripts were quantified for each gene (Fig. 5). When comparing the sense and antisense reads in IB at day 5 and day 7, we observed a relatively higher level of sense transcripts compared to antisense in *ftsZ* and *ctrA* and conversely a higher level of antisense in *folC*. The sense:antisense ratio was around 1 for *spoT, ank12_01,* and *scaD* on both day 5 and day 7. Similar ratios were observed in EB taken on both days, although in this case, there was also a higher level of sense transcripts than antisense transcripts in *spoT,* although not statistically significant. Across *ftsZ, ctrA, spoT,* and *ank12_01,* the sense:antisense ratio decreased between day 5 and day 7 in EB, although this difference was not always statistically significant.

We next compared the ratios between IB and EB populations. For *ftsZ, ctrA, ank12_01, scaD,* and *folC,* overall transcript levels were lower in EB compared with IB, and the sense:antisense ratios were similar between IB and EB at both time points. By contrast, in *folC,* overall transcript levels were also reduced, but there was an increased sense:antisense ratio in EB compared with IB at each time point. This indicates a reduction in antisense transcription in extracellular bacteria.

DISCUSSION

Here, we report the first detailed characterization of antisense transcription in Ot. We sought to examine whether the low sense:antisense ratio previously reported in RNA sequencing studies was a result of pervasive nonspecific transcription resulting from an AT-rich genome or whether it was driven by specific processes in individual genes. To address this question, we carried out a large analysis of RNA sequencing data in multiple Ot strains. Examination of the transcript distribution revealed numerous genes with low sense:antisense ratios containing highly conserved antisense peaks in specific regions

Downloaded from https://journals.asm.org/journal/jb on 21 August 2026 by 131.111.184.205.

Downloaded from https://journals.asm.org/journal/jb on 21 August 2026 by 131.111.184.205.

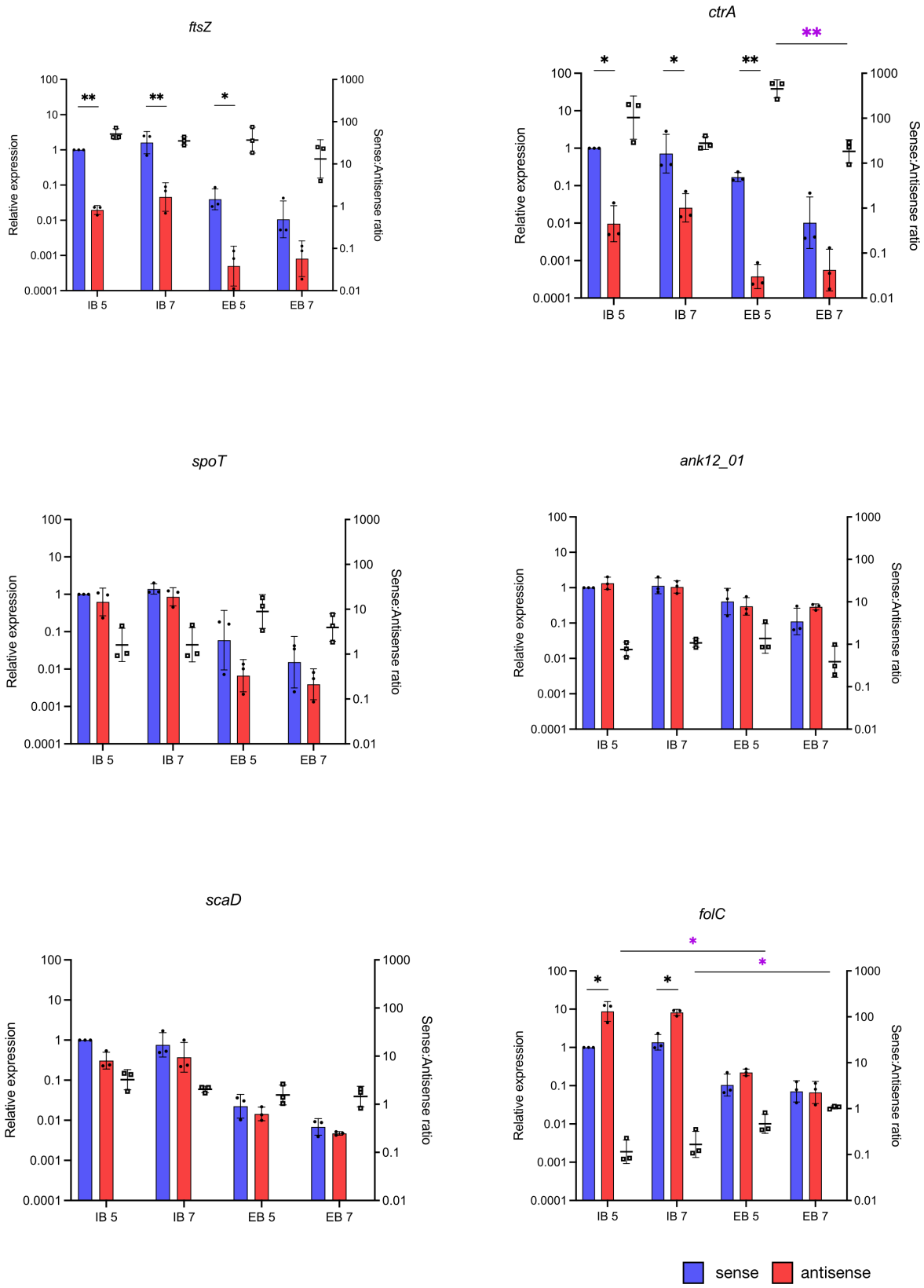


FIG 5 Quantification of the sense/antisense ratio at different time points in the bacterial infection cycle. RNA was isolated from bacteria during rapid growth (5 days post-infection) and at last stages of infection (7 days post-infection). Intracellular bacteria (IB) and those that had already exited from infected cells (EB) were isolated separately. The relative levels of sense and antisense transcripts were measured for each gene at each time point using RT-qPCR with primers from the

(Continued on next page)

Fig 5 (Continued)

region selected in Fig. 4. Transcripts were normalized to the Ot DNA copy number of IB 5-dpi sample. The graph shows the relative expression on the left y-axis, and the sense:antisense ratio for each sample type/time point is shown on the right y-axis. The graph shows quantification of sense and antisense transcripts as well as the ratio of these values. The results of three independent biological replicates are shown, with mean and standard deviation. Statistical significance was determined using a standard *t* test with Welch correction, where ns indicates no significant difference, * indicates *P*-value ≤ 0.05; ** *P*-value ≤ 0.01. The black asterix compares relative expression, while the magenta asterix compares the sense:antisense ratio.

of the gene. Four of five antisense RNAs examined were independently detected by Northern blotting, confirming the existence of discrete antisense transcripts. In genes *karp_02209, ank12_01,* and *scaD,* the band was larger than that predicted by RNA-seq, suggesting that RNA-seq only identified a shorter region within larger antisense RNA transcripts. No band was detected by Northern blot analysis of *folC,* which may be explained by the presence of antisense transcripts with low abundance or short half-life or the lower sensitivity of Northern blot analysis compared with RT-qPCR. The identification of discrete and conserved regions of antisense transcription suggests the possible presence of a specific promoter driving antisense transcription that may inhibit gene expression through *cis*-inhibition of the coding RNA strand. Similar dedicated antisense bacterial promoters have been described in other bacterial systems, including toxin/antitoxin systems, and are particularly important in regulating plasmid replication and conjugation (34, 36). It is notable that two of the genes with consistently high antisense expression across all strains encoded genes in the phage-like gene transfer agent of Ot. While the activity of this agent has not been experimentally shown, its conserved presence in a highly reduced genome suggests it is functional, and it may be regulated by antisense transcription. Notably, high antisense transcription was recently reported in a related bacterium *Wolbachia,* especially in phage genes, reminiscent of our current observations (37).

PCR quantification of the sense and antisense transcripts in different regions within a gene revealed significant differences in the magnitude of sense transcripts as well as the sense:antisense ratio. Differences in the sense transcript may result from the presence of incomplete or partially degraded transcripts, but it could also reflect differences in the efficiency of nested PCR primers for that region. Since the same nested primers are used for sense and antisense transcripts, the ratio will not be affected. *cis*-antisense transcription can initiate from multiple sites within a gene, and this is shown by the presence of specific antisense peaks in RNA sequencing reads as well as differences in the sense: antisense ratio at different regions within a gene in the PCR amplification experiment. *folC* exhibited a single, conserved antisense peak in RNA sequencing data, but this did not correlate with a single region of particularly high sense: antisense on the PCR assay. This discrepancy may be accounted for by the different cell types used or the greater sensitivity of PCR to detect antisense transcripts compared with RNA sequencing.

The EB population of Ot is significantly different from IB. Due to its extracellular location, it lacks access to essential nutrients and thus cannot replicate. Total RNA levels are extremely low, and it is not known whether there remains residual transcriptional activity. The small amount of RNA present may derive from stable transcripts generated during the previous IB stage or from ongoing, low-level transcriptional activity. A comparison of the sense:antisense ratio in IB and EB revealed that ratios remained broadly similar in most genes, with the exception of the one gene with a clearly defined antisense transcript, *folC*, where a significant increase in the sense:antisense ratio was observed in the extracellular form compared with the intracellular form of bacteria. This may reflect differential half-life of sense and antisense transcripts, with sense transcripts being specifically protected from degradation during the EB stage of development.

In summary, we have shown that numerous Ot genes exhibit high antisense transcript levels and that in 19 genes, these are conserved between strains. This study lays the foundation for further studies on the regulation of gene expression of Ot as well as the physiology of the EB Ot population.

Downloaded from https://journals.asm.org/journal/jb on 21 August 2026 by 131.111.184.205.

MATERIALS AND METHODS

Mammalian cell culture

All experiments were performed using the mouse fibroblast cell line L929 (ECACC 85011425). The cells were grown in DMEM (Gibco 11965092) supplemented with 10% FBS (Sigma-Aldrich F7524) at 37°C and 5% CO_2. The cells were seeded at 1.2×10^6 cells per T75 flask 2 days prior to infection with bacteria.

Bacterial propagation

L929 cells were infected with Ot strain Karp at a multiplicity of infection (MOI) of 200:1. The Karp-infected L929 cells were then maintained at 35°C and 5% CO_2 until the required day of harvest. Purified Karp stocks were stored in SPG solution (218 mM sucrose, 3.76 mM KH_2PO_4, 7.1 mM K_2HPO_4, and 4.9 mM potassium glutamate) at −80°C prior to use.

Analysis of antisense transcription from the RNA sequencing data set

Orientia-infected human umbilical vein endothelial cells (HUVEC) dual RNA-seq reads were downloaded from the sequence read archive (SRA) from project number PRJNA1047511 and GEO entry GSE139498. These data have been previously described (32, 33). Briefly, cDNA for GSE139498 (Karp and UT176) was prepared by Vertis Biosciences, with RNA fragmented by sonication to generate 200–400 bp fragments, ligated to Illumina TruSeq adapters, and purified by Agencourt AMPure XP bead purification before sequencing on a NextSeq 500. For PRJNA1047511 (all other strains), the Core Unit Sysmed at the University of Würzburg prepared cDNA using the Corall Total RNA Library Prep kit, generating fragments in the 200–600 bp range before sequencing on a NextSeq 2000. In both protocols, an adapter is ligated to the 3′ end of the first-strand cDNA before PCR amplification, preserving strand information.

RNA-seq read processing and alignment

Quality control of sequencing reads was performed using FastQC (https://www.bioinformatics.babraham.ac.uk/projects/fastqc/) and BBDuk (https://PRJNA1047511bbmap.org/), removing low-quality reads, primers, and adapters.

To generate a bam file for each Ot strain, reads were aligned to a concatenated human (Gencode v38) and bacterial genome with Bowtie2 (38) using *--local* alignment and Samtools (39) for sorting and indexing.

Genome coverage tracks

The bamCoverage script from DeepTools (40) was used to generate coverage files for forward and reverse stranded reads, using parameters of *--binSize 5 --filterRNAstrand forward/reverse --outFileFormat bigwig*. The Integrative Genomics Viewer (IGV) (41) was used to manually generate genome tracks for each gene from each of the eight bacterial genomes, which were then combined with Adobe Illustrator. All bacterial genome and annotation files that were used in this study were taken directly from Hayward et al (33).

Antisense peak calling

CSaw (42) is used to identify antisense peaks using *window size 50*, *spacing 50*, *read length 75*, and *minq 10*, removing duplicated reads and excluding forward-facing reads. For each strain, peaks were normalized using CPM and then identified in each of the three replicates separately (to ensure the peaks we are using are not background signals and/or artifacts). Adjacent bins from CSaw output were merged using the *reduce* function from GenomicRanges (43). Consensus peaks were then determined if the peak was identified across all three replicates, using findOverlaps and intersect from GenomicRanges (43). Peaks containing at least 200 reads were retained for further analysis.

Downloaded from https://journals.asm.org/journal/jb on 21 August 2026 by 131.111.184.205.

Downloaded from https://journals.asm.org/journal/jb on 21 August 2026 by 131.111.184.205.

Coverage plots for Fig. 2A

A custom script was created that used Samtools (39) to extract the number of reads (coverage) for each of the specified locus tags for each strain, determining the coverage of forward and reverse reads from the three replicates.

PCR assay

The RNA of purified Ot was extracted using the Qiagen RNeasy Plus kit (Qiagen 74136) according to the manufacturer's instructions. To avoid DNA contamination, the total RNA (5 µg) was incubated with TURBO DNase (ThermoFisher AM2238) at 37°C for 4 h before use in other PCR assays. The RNA samples were then reverse-transcribed to cDNA using ImProm-II reverse transcriptase (Promega A3802) and specific primers (sense primers and antisense primers for each target region) (Table S2). cDNA synthesis was also performed on RNA samples without the addition of a specific primer to detect the background amplification and on RNA samples without reverse transcriptase to ensure that there was no DNA contamination in the RNA samples. The resulting cDNA was then used as template for PCR using GoTaq DNA Polymerase (Promega M3001) and nested primers for *ftsZ*, *ctrA*, *spoT*, *ank12_01*, *folC*, and *scaD*. The nested PCR products for sense and antisense expression were compared by gel electrophoresis and Gel Doc EZ System (Bio-Rad 1708270 and 1708273, respectively). The band intensities were then quantified by ImageJ software (ImageJ v1.54d).

RT-qPCR

The cDNA used in the PCR assay was diluted 1:10, and 1 µL was used as the template for qPCR using qPCRBIO SyGreen Mix Lo-ROX (PB20.11) with primers for each target region (Table S2). The amount of RNA used for reverse transcription in each sample was normalized relative to the Ot copy number in the 5-dpi IB sample to ensure equivalent bacterial input. Gene expression data were analyzed using the $2^{-\Delta\Delta Ct}$ method and were compared relative to the sense transcript of the IB sample.

Northern blot

Total RNA was extracted from Karp at 5 dpi, and approximately 10 µg of RNA was resolved on a 1.5% agarose gel containing 2% formaldehyde. Gel electrophoresis was performed in 1× MOPS running buffer (20 mM MOPS, 5 mM sodium acetate, and 2 mM EDTA), and RNA samples were mixed with 20 µL of the loading dye (50% formamide, 6.142% formaldehyde, 1× MOPS, 10% glycerol, and 0.05% bromophenol blue) prior to loading. RNA was then transferred to a positively charged nylon membrane (Roche, 11417240001) by capillary transfer using 20× SSC buffer (3 M NaCl and 0.3 M sodium citrate, at pH = 7) overnight. RNA was subsequently fixed to the membrane by baking at 80°C for 2 h.

For probe preparation, approximately 5 ug of total RNA was reverse-transcribed using the UltraScript 2.0 cDNA Synthesis Kit (PCRBIOSYSTEMS, PB30.32) with gene-specific sense primers targeting *K_02209*, *K_00287*, *folC*, *ank12_01*, and *scaD*. The resulting cDNA was then PCR-amplified using Q5 DNA polymerase (M0491L) with specific primers to make DNA templates incorporating a T7 RNA polymerase promoter sequence. DIG-labeled RNA probes were synthesized by *in vitro* transcription reaction with digoxigenin-11-UTP and T7 RNA polymerase from the DIG northern starter kit (Roche, 12039672910) according to the manufacturer's instructions.

Hybridization was carried out in hybridization buffer (DIG Easy Hyb Granules) at 65°C overnight with gentle agitation. The membrane was subsequently washed under the following conditions: Wash I (2× SSC, 0.1% SDS) at 20°C, Wash II (0.1× SSC, 0.1% SDS) at 65°C, and Wash III (0.1 M maleic acid, 0.15 M NaCl, and 0.3% Tween-20, at pH 7.5) at room temperature. The membrane was then incubated in blocking solution followed by antibody solution containing anti-digoxigenin-AP antibody in blocking buffer (1:10,000 dilution), each for 30 min at room temperature. Detection was performed using the

CDP-Star substrate, and chemiluminescent signals were captured using a ChemiDoc MP imaging system (Bio-Rad, 734BR5238).

Preparation of IB and EB bacteria

Ot were isolated from L929 cells on 4, 5, and 7 dpi. For EB isolation, the supernatant portion of the culture was transferred to a 50-mL centrifuge tube and centrifuged at 1,000 rpm, 4°C for 5 min to remove host cells. The supernatant was then transferred into a new 50-mL centrifuge tube and centrifuged at 20,000 × *g*, 4°C for 15 min to collect EB pellets. For IB isolation, 1.5 ml of fresh DMEM was added to the culture flasks. Ot-infected host cells on the adhering surface were then scraped and transferred into 2-mL microcentrifuge tubes. The microcentrifuge tubes were then placed into Next Advance Bullet Blander (BBY24M-0710977) and homogenized at speed 8 for 2 min to break host cells and release IB from host cells. The cell suspensions were then centrifuged at 300 × *g*, RT for 3 min to remove host cells. The supernatants were then transferred into new 1.5-mL microcentrifuge tubes and centrifuged at 20,000 × *g*, at RT for 3 min to collect IB pellets. Both IB and EB pellets were then resuspended in RNAprotect Bacteria Reagent (QIAGEN 76506) in a ratio of 2:1 (volume of RNA protect to volume of the Ot pellet) and stored at −80°C until used. Hotshot was performed to quantify IB and EB DNA concentration. A portion of IB and EB cell suspension (50 uL) was pelleted and heated in 25 uL lysis buffer solution (25 mM NaOH and 0.2 mM EDTA) at 95°C for 30 min. The lysed solution is then added with 25 uL neutralization buffer (40 mM Tris-HCl) and stored at −20°C or directly used as a template in qPCR. Amplification was performed on Bio-Rad CFX96 (CT008648) using qPCRBIO Probe Mix Lo-ROX (PCR Biosystems PB20.21), 47-kDa probe ([6-FAM]-TTCCACATTGTGCTGCAGATCCTTC-[TAMRA]), 47-kDa forward primer (TCC AGAATTAAATGAGAATTTAGGAC), and 47-kDa reverse primer (TTAGTAATTACATCTCCAGG AGCAA). The quantification of Ot copy number was then determined in relative to the 47-kDa standard curve.

Statistical analysis

The statistical analyses for band intensity were carried out using GraphPad Prism version 10.4.2 (633). A standard *t* test with Welch correction was used to compare relative expression between two sample groups.

Downloaded from https://journals.asm.org/journal/jb on 21 August 2026 by 131.111.184.205.

AUTHOR AFFILIATIONS

[1]Faculty of Tropical Medicine, Mahidol-Oxford Tropical Medicine Research Unit, Mahidol University, Bangkok, Thailand
[2]Helmholtz Institute for RNA-based Infection Research (HIRI), Helmholtz Centre for Infection Research (HZI), Würzburg, Germany
[3]Department of Biology, University of Toronto, Mississauga, Canada
[4]Department of Cell and Systems Biology, University of Toronto, Toronto, Canada
[5]Department of Biochemistry, University of Cambridge, Cambridge, United Kingdom
[6]Department of Pathology, University of Cambridge, Cambridge, United Kingdom
[7]Cambridge Institute for Medical Research, University of Cambridge, Cambridge, United Kingdom

AUTHOR ORCIDs

Lars Barquist http://orcid.org/0000-0003-4732-2667
Jeanne Salje http://orcid.org/0000-0001-5802-4580

FUNDING

Funder	Grant(s)	Author(s)
Wellcome Trust	224277/Z/21/Z	Jeanne Salje

AUTHOR CONTRIBUTIONS

Chitrasak Kullapanich, Formal analysis, Investigation | Regan Hayward, Formal analysis | Lars Barquist, Formal analysis, Supervision, Writing – review and editing | Jeanne Salje, Supervision, Writing – original draft

DATA AVAILABILITY

The RNA-seq data used in this analysis are available on the sequence read archive (SRA) from project number PRJNA1047511 (33) (Gilliam, TA763, Kato, UT76, TA686, Karp, and Ikeda) and on GEO from entry GSE139498 (32) (Karp, UT176).

ADDITIONAL FILES

The following material is available online.

Supplemental Material

Supplemental figure (JB00564-25-s0001.tiff). Fig. S1.
Supplemental tables (JB00564-25-s0002.xlsx). Tables S1 to S11.

REFERENCES

1. Luce-Fedrow A, Lehman ML, Kelly DJ, Mullins K, Maina AN, Stewart RL, Ge H, John HS, Jiang J, Richards AL. 2018. A review of scrub typhus (*Orientia tsutsugamushi* and related organisms): then, now, and tomorrow. Trop Med Infect Dis 3:8. https://doi.org/10.3390/tropicalmed3010008
2. Khairkar M, Vagha S, Deotale V. 2023. Review on scrub typhus: an important etiology of acute undifferentiated fever illness. Cureus 15:e47290. https://doi.org/10.7759/cureus.47290
3. Weitzel T, Dittrich S, López J, Phuklia W, Martinez-Valdebenito C, Velásquez K, Blacksell SD, Paris DH, Abarca K. 2016. Endemic scrub typhus in South America. N Engl J Med 375:954–961. https://doi.org/10.1056/NEJMoa1603657
4. Abarca K, Martínez-Valdebenito C, Angulo J, Jiang J, Farris CM, Richards AL, Acosta-Jamett G, Weitzel T. 2020. Molecular description of a novel *Orientia* species causing scrub typhus in Chile. Emerg Infect Dis 26:2148–2156. https://doi.org/10.3201/eid2609.200918
5. Izzard L, Fuller A, Blacksell SD, Paris DH, Richards AL, Aukkanit N, Nguyen C, Jiang J, Fenwick S, Day NPJ, Graves S, Stenos J. 2010. Isolation of a novel *Orientia* species (*O. chuto* sp. nov.) from a patient infected in Dubai. J Clin Microbiol 48:4404–4409. https://doi.org/10.1128/JCM.01526-10
6. Bonell A, Lubell Y, Newton PN, Crump JA, Paris DH. 2017. Estimating the burden of scrub typhus: a systematic review. PLoS Negl Trop Dis 11:e0005838. https://doi.org/10.1371/journal.pntd.0005838
7. Ge Y, Rikihisa Y. 2011. Subversion of host cell signaling by *Orientia tsutsugamushi*. Microbes Infect 13:638–648. https://doi.org/10.1016/j.micinf.2011.03.003
8. Salje J. 2021. Cells within cells: Rickettsiales and the obligate intracellular bacterial lifestyle. Nat Rev Microbiol 19:375–390. https://doi.org/10.1038/s41579-020-00507-2
9. Kim SW, Ihn KS, Han SH, Seong SY, Kim IS, Choi MS. 2001. Microtubule- and dynein-mediated movement of *Orientia tsutsugamushi* to the microtubule organizing center. Infect Immun 69:494–500. https://doi.org/10.1128/IAI.69.1.494-500.2001
10. Manigrasso G, Saharat K, Chaichana P, Kullapanich C, Atwal S, Boulanger J, Morgan TE, Kramer H, Salje J, Carter AP. 2025. The intracellular bacterium *Orientia tsutsugamushi* uses the autotransporter ScaC to activate BICD adaptors for dynein-based motility. Nat Commun 16:6122. https://doi.org/10.1038/s41467-025-61105-5
11. Rikihisa Y, Ito S. 1979. Intracellular localization of *Rickettsia tsutsugamushi* in polymorphonuclear leukocytes. J Exp Med 150:703–708. https://doi.org/10.1084/jem.150.3.703
12. Rikihisa Y, Ito S. 1980. Localization of electron-dense tracers during entry of *Rickettsia tsutsugamushi* into polymorphonuclear leukocytes. Infect Immun 30:231–243. https://doi.org/10.1128/iai.30.1.231-243.1980
13. Gillespie JJ, Salje J. 2023. *Orientia* and *Rickettsia*: different flowers from the same garden. Curr Opin Microbiol 74:102318. https://doi.org/10.1016/j.mib.2023.102318
14. Atwal S, Wongsantichon J, Giengkam S, Saharat K, Pittayasathornthun YJ, Chuenklin S, Wang LC, Chung T, Huh H, Lee S-H, Sobota RM, Salje J. 2022. The obligate intracellular bacterium *Orientia tsutsugamushi* differentiates into a developmentally distinct extracellular state. Nat Commun 13:3603. https://doi.org/10.1038/s41467-022-31176-9
15. Cho N-H, Kim H-R, Lee J-H, Kim S-Y, Kim J, Cha S, Kim S-Y, Darby AC, Fuxelius H-H, Yin J, Kim JH, Kim J, Lee SJ, Koh Y-S, Jang W-J, Park K-H, Andersson SGE, Choi M-S, Kim I-S. 2007. The *Orientia tsutsugamushi* genome reveals massive proliferation of conjugative type IV secretion system and host-cell interaction genes. Proc Natl Acad Sci USA 104:7981–7986. https://doi.org/10.1073/pnas.0611553104
16. Nakayama K, Yamashita A, Kurokawa K, Morimoto T, Ogawa M, Fukuhara M, Urakami H, Ohnishi M, Uchiyama I, Ogura Y, Ooka T, Oshima K, Tamura A, Hattori M, Hayashi T. 2008. The Whole-genome sequencing of the obligate intracellular bacterium *Orientia tsutsugamushi* revealed massive gene amplification during reductive genome evolution. DNA Res 15:185–199. https://doi.org/10.1093/dnares/dsn011
17. Batty EM, Chaemchuen S, Blacksell S, Richards AL, Paris D, Bowden R, Chan C, Lachumanan R, Day N, Donnelly P, Chen S, Salje J. 2018. Long-read whole genome sequencing and comparative analysis of six strains of the human pathogen *Orientia tsutsugamushi*. PLoS Negl Trop Dis 12:e0006566. https://doi.org/10.1371/journal.pntd.0006566
18. Giengkam S, Kullapanich C, Wongsantichon J, Adcox HE, Gillespie JJ, Salje J. 2023. *Orientia tsutsugamushi:* comprehensive analysis of the mobilome of a highly fragmented and repetitive genome reveals the capacity for ongoing lateral gene transfer in an obligate intracellular bacterium. mSphere 8:e0026823. https://doi.org/10.1128/msphere.00268-23
19. Gillespie JJ, Joardar V, Williams KP, Driscoll T, Hostetler JB, Nordberg E, Shukla M, Walenz B, Hill CA, Nene VM, Azad AF, Sobral BW, Caler E. 2012. A *Rickettsia* genome overrun by mobile genetic elements provides insight into the acquisition of genes characteristic of an obligate intracellular lifestyle. J Bacteriol 194:376–394. https://doi.org/10.1128/JB.06244-11
20. Ogata H, La Scola B, Audic S, Renesto P, Blanc G, Robert C, Fournier P-E, Claverie J-M, Raoult D. 2006. Genome sequence of *Rickettsia bellii* illuminates the role of amoebae in gene exchanges between intracellular pathogens. PLoS Genet 2:e76. https://doi.org/10.1371/journal.pgen.0020076
21. Blanc G, Ogata H, Robert C, Audic S, Claverie J-M, Raoult D. 2007. Lateral gene transfer between obligate intracellular bacteria: evidence from the *Rickettsia massiliae* genome. Genome Res 17:1657–1664. https://doi.org/10.1101/gr.6742107

Downloaded from https://journals.asm.org/journal/jb on 21 August 2026 by 131.111.184.205.

22. Londoño AF, Mendell NL, Valbuena GA, Routh AL, Wood TG, Widen SG, Rodas JD, Walker DH, Bouyer DH. 2019. Whole-genome sequence of *Rickettsia parkeri* strain atlantic rainforest, isolated from a Colombian tick. Microbiol Resour Announc 8:e00684-19. https://doi.org/10.1128/MRA.00684-19
23. Gillespie JJ, Driscoll TP, Verhoeve VI, Utsuki T, Husseneder C, Chouljenko VN, Azad AF, Macaluso KR. 2014. Genomic diversification in strains of *Rickettsia felis* Isolated from different arthropods. Genome Biol Evol 7:35–56. https://doi.org/10.1093/gbe/evu262
24. Felsheim RF, Kurtti TJ, Munderloh UG. 2009. Genome sequence of the endosymbiont *Rickettsia peacockii* and comparison with virulent *Rickettsia rickettsii*: identification of virulence factors. PLoS One 4:e8361. https://doi.org/10.1371/journal.pone.0008361
25. Millar JA, Raghavan R. 2020. Modulation of bacterial fitness and virulence through antisense RNAs. Front Cell Infect Microbiol 10:596277. https://doi.org/10.3389/fcimb.2020.596277
26. Thomason MK, Storz G. 2010. Bacterial antisense RNAs: how many are there, and what are they doing? Annu Rev Genet 44:167–188. https://doi.org/10.1146/annurev-genet-102209-163523
27. Ma C, Simons RW. 1990. The IS10 antisense RNA blocks ribosome binding at the transposase translation initiation site. EMBO J 9:1267–1274. https://doi.org/10.1002/j.1460-2075.1990.tb08235.x
28. Ellis MJ, Trussler RS, Haniford DB. 2015. Hfq binds directly to the ribosome-binding site of IS10 transposase mRNA to inhibit translation. Mol Microbiol 96:633–650. https://doi.org/10.1111/mmi.12961
29. Liao SM, Wu TH, Chiang CH, Susskind MM, McClure WR. 1987. Control of gene expression in bacteriophage P22 by a small antisense RNA. I. Characterization *in vitro* of the Psar promoter and the sar RNA transcript. Genes Dev 1:197–203. https://doi.org/10.1101/gad.1.2.197
30. Georg J, Hess WR. 2011. Cis-antisense RNA, another level of gene regulation in bacteria. Microbiol Mol Biol Rev 75:286–300. https://doi.org/10.1128/MMBR.00032-10
31. Lloréns-Rico V, Cano J, Kamminga T, Gil R, Latorre A, Chen W-H, Bork P, Glass JI, Serrano L, Lluch-Senar M. 2016. Bacterial antisense RNAs are mainly the product of transcriptional noise. Sci Adv 2:e1501363. https://doi.org/10.1126/sciadv.1501363
32. Mika-Gospodorz B, Giengkam S, Westermann AJ, Wongsantichon J, Kion-Crosby W, Chuenklin S, Wang LC, Sunyakumthorn P, Sobota RM, Subbian S, Vogel J, Barquist L, Salje J. 2020. Dual RNA-seq of *Orientia tsutsugamushi* informs on host-pathogen interactions for this neglected intracellular human pathogen. Nat Commun 11:3363. https://doi.org/10.1038/s41467-020-17094-8
33. Hayward R, Chuenklin S, Kullapanich C, Chaichana P, Ferguson B, Barquist L, Salje J. 2025. Comparative dual RNA-Seq analysis of seven *Orientia tsutsugamushi* strains in endothelial cells reveals regulatory patterns in bacterial and host pathways during infection. bioRxiv. https://doi.org/10.1101/2025.12.01.691569
34. Gerdes K, Wagner EGH. 2007. RNA antitoxins. Curr Opin Microbiol 10:117–124. https://doi.org/10.1016/j.mib.2007.03.003
35. Brantl S, Müller P. 2021. Cis- and trans-encoded small regulatory RNAs in *Bacillus subtilis*. Microorganisms 9:1865. https://doi.org/10.3390/microorganisms9091865
36. Berk JM, Lee MJ, Zhang M, Lim C, Hochstrasser M. 2022. OtDUB from the human pathogen *Orientia tsutsugamushi* modulates host membrane trafficking by multiple mechanisms. Mol Cell Biol 42:e0007122. https://doi.org/10.1128/mcb.00071-22
37. Suliman Y, Li Z, Sinha A, Dyer PD, Hartley CS, Ettwiller L, Darby AC, Carlow CK, Makepeace BL. 2025. Erratum: Cappable-seq reveals the transcriptional landscape of stress responses in the bacterial endosymbiont *Wolbachia*. Microb Genom 11. https://doi.org/10.1099/mgen.0.001584
38. Langmead B, Salzberg SL. 2012. Fast gapped-read alignment with Bowtie 2. Nat Methods 9:357–359. https://doi.org/10.1038/nmeth.1923
39. Danecek P, Bonfield JK, Liddle J, Marshall J, Ohan V, Pollard MO, Whitwham A, Keane T, McCarthy SA, Davies RM, Li H. 2021. Twelve years of SAMtools and BCFtools. Gigascience 10:giab008. https://doi.org/10.1093/gigascience/giab008
40. Ramírez F, Dündar F, Diehl S, Grüning BA, Manke T. 2014. deepTools: a flexible platform for exploring deep-sequencing data. Nucleic Acids Res 42:W187–W191. https://doi.org/10.1093/nar/gku365
41. Robinson JT, Thorvaldsdóttir H, Winckler W, Guttman M, Lander ES, Getz G, Mesirov JP. 2011. Integrative genomics viewer. Nat Biotechnol 29:24–26. https://doi.org/10.1038/nbt.1754
42. Lun ATL, Smyth GK. 2016. Csaw: a bioconductor package for differential binding analysis of ChIP-seq data using sliding windows. Nucleic Acids Res 44:e45. https://doi.org/10.1093/nar/gkv1191
43. Lawrence M, Huber W, Pagès H, Aboyoun P, Carlson M, Gentleman R, Morgan MT, Carey VJ. 2013. Software for computing and annotating genomic ranges. PLoS Comput Biol 9:e1003118. https://doi.org/10.1371/journal.pcbi.1003118

Downloaded from https://journals.asm.org/journal/jb on 21 August 2026 by 131.111.184.205.